Science of the Total Environment 934 (2024) 173046

Contents lists available at ScienceDirect

Science of the Total Environment

journal homepage: www.elsevier.com/locate/scitotenv

Solid phase speciation controls copper mobilisation from marine sediments by methanobactin

Danielle D. Rushworth [a,b,1], Walter D.C. Schenkeveld [c,*], Naresh Kumar [c,*], Vincent Noël [d], Jannes Dewulf [b], Niels A.G.M. van Helmond [e,f], Caroline P. Slomp [e,f], Moritz F. Lehmann [g], Stephan M. Kraemer [a]

[a] Centre for Microbiology and Environmental Systems Science, University of Vienna, Vienna, Austria
[b] Environmental Sciences, Copernicus Institute of Sustainable Development, Utrecht University, Utrecht, Netherlands
[c] Soil Chemistry and Chemical Soil Quality, Environmental Sciences, Wageningen University, Wageningen, Netherlands
[d] Environmental Geochemistry Group at SLAC, Stanford Synchrotron Radiation Lightsource (SSRL), SLAC National Accelerator Laboratory, Menlo Park, USA
[e] Geochemistry, Department of Earth Sciences, Utrecht University, Utrecht, Netherlands
[f] Department of Microbiology, Radboud Institute for Biological and Environmental Sciences, Radboud University, Nijmegen, Netherlands
[g] Department of Environmental Sciences, University of Basel, Basel, Switzerland

HIGHLIGHTS

- The chalkophore methanobactin (mb) can mobilise Cu from sulphidic marine sediments.
- Cu sulphide mineralogy limits Cu mobilisation by mb to sediments bearing CuS.
- A high porosity in surface sediments limits mb adsorption and favors Cu mobilisation.

GRAPHICAL ABSTRACT

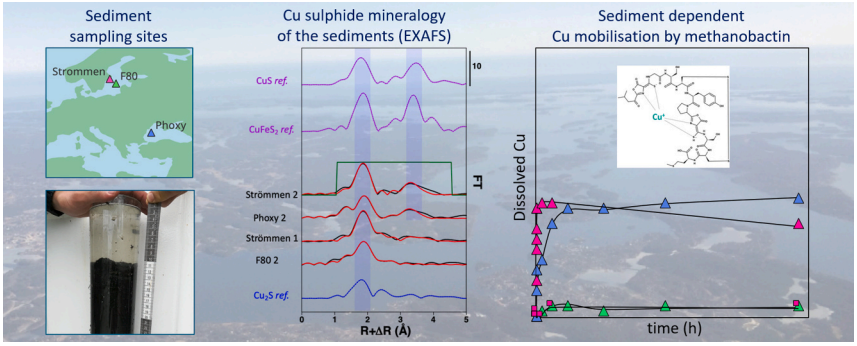

ARTICLE INFO

Editor: Daniel Alessi

Keywords:
Biological Cu acquisition
Chalkophores
Sulphide minerals
Ligand-enhanced metal mobilisation
Adsorption
Methanotrophs

ABSTRACT

Although marine environments represent huge reservoirs of the potent greenhouse gas methane, they currently contribute little to global net methane emissions. Most of the methane is oxidized by methanotrophs, minimizing escape to the atmosphere. Aerobic methanotrophs oxidize methane mostly *via* the copper (Cu)-bearing enzyme particulate methane monooxygenase (pMMO). Therefore, aerobic methane oxidation depends on sufficient Cu acquisition by methanotrophs. Because they require both oxygen and methane, aerobic methanotrophs reside at oxic-anoxic interfaces, often close to sulphidic zones where Cu bioavailability can be limited by poorly soluble Cu sulphide mineral phases. Under Cu-limiting conditions, certain aerobic methanotrophs exude Cu-binding ligands termed chalkophores, such as methanobactin (mb) exuded by *Methylosinus trichosporium* OB3b. Our main

* Corresponding authors.
E-mail addresses: walter.schenkeveld@wur.nl (W.D.C. Schenkeveld), naresh.kumar@wur.nl (N. Kumar).
[1] Present address: Department of Earth Sciences, University of Delaware, Newark, Delaware, USA.

https://doi.org/10.1016/j.scitotenv.2024.173046
Received 6 February 2024; Received in revised form 26 April 2024; Accepted 5 May 2024
Available online 11 May 2024
0048-9697/© 2024 The Authors. Published by Elsevier B.V. This is an open access article under the CC BY license (http://creativecommons.org/licenses/by/4.0/).

objective was to establish whether chalkophores can mobilise Cu from Cu sulphide-bearing marine sediments to enhance Cu bioavailability.

Through a series of kinetic batch experiments, we investigated Cu mobilisation by mb from a set of well-characterized sulphidic marine sediments differing in sediment properties, including Cu content and phase distribution. Characterization of solid-phase Cu speciation included X-ray absorption spectroscopy and a targeted sequential extraction. Furthermore, in batch experiments, we investigated to what extent adsorption of metal-free mb and Cu-mb complexes to marine sediments constrains Cu mobilisation.

Our results are the first to show that both solid phase Cu speciation and chalkophore adsorption can constrain methanotrophic Cu acquisition from marine sediments. Only for certain sediments did mb addition enhance dissolved Cu concentrations. Cu mobilisation by mb was not correlated to the total Cu content of the sediment, but was controlled by solid-phase Cu speciation. Cu was only mobilised from sediments containing a mono-Cu-sulphide (CuS_x) phase. We also show that mb adsorption to sediments limits Cu acquisition by mb to less compact (surface) sediments. Therefore, in sulphidic sediments, mb-mediated Cu acquisition is presumably constrained to surface-sediment interfaces containing mono-Cu-sulphide phases.

1. Introduction

Marine sediments hold ~500–2500 Gt of the potent greenhouse gas methane (CH_4) (Milkov, 2004; Reeburgh, 2007), which has a ~25 times larger global warming potential over 100 years than carbon dioxide (Hartmann et al., 2014). Yet, marine environments emit only 0.02 Gt of methane to the atmosphere per year (3–3.5 % of total global emissions) (Kirschke et al., 2013), because methane emissions are mitigated by the "microbial methane filter" (Knittel and Boetius, 2009; Niemann et al., 2006; Steeb et al., 2014; Wallenius et al., 2021). In marine environments, the microbial methane filter primarily involves anaerobic oxidation of methane (AOM), performed by a consortium of sulphate-reducing bacteria and methanotrophic archaea (Boetius et al., 2000), and aerobic methane oxidation (MOx), performed by methanotrophic bacteria (aerobic methanotrophs) (Boetius and Wenzhöfer, 2013). While AOM reduces methane concentrations before they reach oxygenated surface sediments and overlying waters, MOx largely prevents the remaining, or "leaked", methane fluxes from reaching the atmosphere.

MOx is catalysed *via* two methane monooxygenase (MMO) enzymes: the copper (Cu)-bearing particulate form (pMMO) and the Fe-bearing soluble form (sMMO) (Hanson and Hanson, 1996; Leak and Dalton, 1986; Murrell et al., 2000). The Cu-bearing pMMO is considered the most efficient enzyme involved in CH_4 oxidation, as expressed by almost all aerobic methanotrophs, and has a higher affinity for methane than sMMO, which is only expressed by a limited group of methanotrophs (Hanson and Hanson, 1996; Leak and Dalton, 1986; Murrell, 2010; Murrell et al., 2000). Therefore, the efficiency of MOx largely depends on the ability of aerobic methanotrophs to acquire Cu from the external environment. Typically, in uncontaminated marine sediments, the average Cu content may range from 25 to 90 μg Cu g^{-1} (dry sediment) (Rudnick and Gao, 2014). Solid-phase Cu is usually comprised of Cu sorbed to mineral surfaces (Parkman et al., 1999), or natural organic matter (NOM) (Christl and Kretzschmar, 2001; Whitby and van den Berg, 2015), and Cu incorporated into Cu-bearing mineral phases (Luther et al., 2002; Shea and Helz, 1989). The binding state of Cu in the solid phase exerts control over its release and often constrains dissolved Cu concentrations and Cu bioavailability (Flemming and Trevors, 1989). In marine waters, total dissolved Cu concentrations can be as low as 10^{-9} M (Bruland, 1980; Coale and Bruland, 1988; Moffett and Dupont, 2007), and free Cu^{2+} concentrations, widely accepted as a measure for the directly bioavailable Cu, reach lower limits as low as 10^{-16} M (Buck and Bruland, 2005; Whitby et al., 2018).

Microbial methane oxidation often occurs close to sulphide-rich, anoxic zones (Durisch-Kaiser et al., 2005; Schouten et al., 2001; Schubert et al., 2006; van Helmond et al., 2018). Cu readily precipitates in the presence of dissolved sulphide, and a significant proportion of the total Cu in reduced marine sediments is likely to be associated with poorly soluble sulphide minerals (Huerta-Diaz and Morse, 1992; Morse, 1994). Numerous Cu sulphide phases of varying stoichiometry, crystallinity, and stability, *e.g.*, the mono-Cu sulphide covellite (CuS) (Shea and Helz, 1989) and the di-Cu sulphide chalcocite (Cu_2S) (Mathur et al., 2018), are found in natural environments. As the relative abundance of Cu in marine sediments is often low compared to other metals, like iron (Fe) (Rudnick and Gao, 2014), Cu can also be structurally incorporated into prominent sulphide phases like pyrite (FeS_2) (Huerta-Diaz and Morse, 1992). Under certain conditions, the secondary Cu—Fe sulphide mineral chalcopyrite ($CuFeS_2$) may also form (Parkman et al., 1999). Despite being thermodynamically unstable in the presence of oxygen, oxidative dissolution of Cu sulphide minerals proceeds extremely slowly (Hoffmann et al., 2020) as evident by observations of Cu sulphide nanoclusters even in oxic marine waters (Luther and Tsamakis, 1989). Aside from Cu sulphide minerals, sulphidised NOM is often observed in sulphidic sediments (Raven et al., 2019) and may also constrain the bioavailability of Cu. During sulphurisation, NOM functional groups like alcohols, ketones, and aldehydes, are transformed to thiol-type groups (Aizenshtat et al., 1995; Schouten et al., 1993) that bind Cu to form very stable Cu-NOM complexes (Leal and Van Den Berg, 1998), which may lower the bioavailable, dissolved fraction of Cu in the vicinity of methanotrophic habitats.

Certain aerobic methanotrophs cope with Cu limitation by exuding strong Cu-binding ligands termed chalkophores, *e.g.*, methanobactin (mb) (DiSpirito et al., 1998; Fitch et al., 1993; Kim et al., 2004). In analogy to siderophores (biogenic ligands exuded by graminaceous plants and microorganisms, particularly under conditions of poor Fe bioavailability (Kraemer et al., 2015)), chalkophores are exuded under conditions of low Cu bioavailability (DiSpirito et al., 1998). Recent studies demonstrated that mb can mobilise mineral-bound Cu (Fru et al., 2011; Kulczycki et al., 2007; Rushworth et al., 2022) and can compete with NOM constituents for the complexation of Cu through fast ligand-exchange reactions (Pesch et al., 2013).

The mechanism of Cu mobilisation by mb from complex environmental matrices like marine sediments is, however, still largely unexplored. To predict the types of environments in which the microbial methane filter might be compromised, there is a necessity to understand how geochemical properties of sediments affect Cu acquisition by aerobic methanotrophs. Differences in solid phase Cu speciation among sediments, *e.g.*, with respect to the crystal structure, stability and redox state of Cu sulphides, are likely to affect the extent of Cu mobilisation by mb in such systems (Rushworth et al., 2022). Also, mobilisation of Cu may be impacted by complexation of competing metal ions, as was observed for phytosiderophores (Schenkeveld et al., 2014a,b, 2017). Despite its very high affinity for Cu, mb can also bind several other metals including Fe, nickel (Ni), cobalt (Co), mercury (Hg), and silver (Ag) (Choi et al., 2006), all of which are found in marine sediments (Crocket et al., 1973; Fitzgerald et al., 2007; Kannan and Falandysz, 1998; van Helmond et al., 2018). Dissolved Fe(II), a byproduct of Fe-mediated AOM and other Fe-reducing microbial redox processes (Egger et al., 2017), can be particularly abundant in the vicinity of zones where MO_x takes place. Finally, potential adsorption of free mb or metal-mb complexes to the solid phase decreases the extent to which Cu is

mobilised and becomes bioavailable. Therefore, the degree to which mb adsorbs to sediment may dictate whether exudation of mb for Cu acquisition is energetically favourable.

The main aim of this study was to investigate Cu mobilisation from natural Cu sulphide-bearing marine sediments in the presence of mb. We hypothesised that mb mobilises Cu from sulphide-bearing marine sediments, but that the extent of mobilisation is influenced by the Cu sulphide mineral phases present within the sediments. Furthermore, we hypothesised that adsorption of free mb and Cu-mb complexes strongly reduces the effectiveness of mb at mobilising Cu from marine sulphide-bearing sediments. To address these hypotheses, sediments with different chemical compositions and from several locations in the Baltic Sea and the Black Sea were selected. While aerobic methanotrophy (relying on Cu-bearing pMMO) may not have occurred at all of these sampling locations, these sediments did allow us to elucidate how naturally occurring Cu sulphides might limit Cu availability for methanotrophs in marine systems. Solid phase Cu speciation in the sediments was thoroughly characterized by X-ray absorption spectroscopy (XAS) and targeted sequential extraction to investigate its effect on Cu mobilisation by mb. Subsequently, kinetic batch experiments were performed in the presence and absence of mb, to examine the mobilisation of Cu and other metals. Finally, the adsorption of free mb and Cu-mb complexes to marine sediments was also investigated.

2. Materials and methods

All reagents used in this study were of analytical grade and were purchased from Carl Roth, VWR, or Merck. Batch experiments were performed in Cellstar® centrifuge tubes. Glassware and non-disposable plastics were acid-washed for >24 h in 1.4 M nitric acid (HNO_3), then rinsed multiple times with ultra-pure water (UPW). All experimental work was done at room temperature (20 ± 1 °C). Solutions for sequential extractions were prepared in O_2-free UPW that was purged with N_2 for >2 h, without boiling.

2.1. Methanobactin

Cu-free mb was isolated and purified from the spent nitrate mineral salts (NMS) growth medium of *Methylosinus trichosporium* OB3b grown in a 9 L fermenter (30 °C) (Whittenbury et al., 1970) containing 0.2 μM $CuCl_2$ following Pesch et al. (2011). Details regarding bacterial cultivation, mb isolation and purification by resin extraction and preparative high pressure liquid chromatography (HPLC; Agilent 1260 Infinity bioinert system) and product characterisation have been reported previously in Rushworth et al. (2022). A Cu-free mb stock solution was prepared by dissolving the freeze-dried isolate (purity: 82–95 %) in UPW. Amber glass-vials were used during purification and the Cu-free mb stock was stored in the dark at −20 °C to avoid (photo)degradation of the product.

2.2. Synthetic Ocean water (SOW)

Synthetic Ocean water (SOW) was prepared anoxically following the procedure for the seawater medium, Aquil (excluding the chelex step), outlined in Sunda et al. (2005). Anoxic UPW (18.2 MΩ cm, TOC < 2 ppb, Milli-Q, Millipore) was prepared by boiling for ~1 h and then purging with nitrogen (N_2) gas for up to 2 h while the water cooled down. Solutes in the stock SOW were prepared at a slightly higher concentration (factor 10/9) than the desired final concentration (Table S1) to allow for the dilution following the addition of treatments, *e.g.*, mb stock solution, during experiments.

2.3. Marine sediments

Sediments from the following three locations were selected, based on differences in their characteristics (including total copper, sulphur, clay and organic carbon content – Table 1): the Fårö Deep in the central Baltic Sea (sediment F80; 58.00000°N, 19.89667°E; Hermans et al., 2019), the Black Sea (sediment Phoxy station 7; 43.89690°N, 29.97652°E; Kraal et al., 2017), and the Stockholm Archipelago (sediment Strömmen; 59.31917°N, 18.11917°E; van Helmond et al., 2020). Sediments were retrieved during several field campaigns, the details of which are outlined in the corresponding studies (Hermans et al., 2019; Kraal et al., 2017; van Helmond et al., 2020). Sediment cores were sliced in the field under anoxic conditions, and sediments were stored at −20 °C until further processing. For each sediment core, three samples taken from different depths below the sediment surface (Table S2) were selected. Samples were named after the sample locations (*i.e.* F80, Phoxy and Strömmen) and numbered 1, 2 or 3, representing various depth intervals below the sediment surface (Table S2). Samples were freeze-dried (under an argon atmosphere), ground using an agate pestle and mortar, and homogenised before further investigation. Other than during freeze-drying, which was performed under a vacuum, sediments were handled in a N_2-filled glove box to avoid oxidation.

2.4. Sediment characterisation

Sediments were characterized using multiple techniques including a targeted sequential extraction procedure, to describe the distribution of Cu over operationally defined pools, and X-ray absorption spectroscopy (XAS) to elucidate the binding environment of Cu in select sediments.

2.4.1. Total elemental contents

Total organic carbon (C_{org}) and nitrogen (N_{org}) contents were quantified using an elemental analyser (Fisons Instruments NA 1500 NCS analyser) following the procedure outlined in van Helmond et al. (2018). Total metal and S contents of the solid phase were quantified using ICP-OES (Perkin Elmer models; Optima 5300 DV and Avio 500) analysis following a triple acid digestion procedure in accordance with van Helmond et al. (van Helmond et al., 2018). Total mercury (Hg) contents were determined using a DMA-80 evo solid mercury analyser. Based on measurement of in-house standards, the recovery of the elements of interest in the total digest was 95–105 %.

2.4.2. Fe, Cu and S speciation determined by sequential extraction

The Cu, Fe and S speciation in the sediments were examined *via* targeted sequential extraction procedures presented in Table S3, where a description of the individual fractions has been included. For Cu speciation, the sequential extraction procedure by Jokinen et al. (2020) was followed; interpretation of the fractions has been adjusted, as explained in the text accompanying Table S3. For Fe, a procedure under a N_2 atmosphere (Table S3), after Kraal et al. (2017) modified from Poulton and Canfield (2005) and Claff et al. (2010) was followed. In this study we also included a "*Residual*" fraction defined as the Total Fe or Cu minus the content extracted in Fractions 1–4 (Table S3). The *Residual* fraction accounted for 0–78 % in the case of Cu and 23–68 % in the case of Fe.

Acid-volatile sulphur (AVS) and chromium reducible sulphur (CRS) (Table S3) were determined by sequential extraction following Burton et al. (2008) and the procedure outlined in Egger et al. (2016). Sulphide was trapped as zinc (Zn) sulphide in a Zn acetate trap solution and quantified *via* iodometric titration.

2.4.3. Cu speciation by XAS

For some of the sediment samples, Cu speciation was additionally assessed by XAS analysis. Cu *K*-edge Extended X-ray Absorption Fine Structure (EXAFS) spectra of sediment samples were collected in fluorescence mode, using a 30-pixel germanium X-ray detector, at 10 K on the 7–3 beamline at Stanford Synchrotron Radiation Lightsource (SSRL). A Si (220) double-crystal monochromator was detuned by 40 % to reject higher harmonic intensity. Bulk ground sediment samples were mounted on a cryostat sample rod inside an N_2-purged glove bag and brought

Table 1
Overview of solid phase sediment characteristics. Clay contents were estimated from the Al content by assuming that clays were present as Al_2SiO_5. Organic C, $CaCO_3$, and Total Fe data for Phoxy sediments were first reported in Kraal et al. (2017), and organic C and $CaCO_3$ for Strömmen sediments were first reported in van Helmond et al. (2020). A table with additional information on sediment characteristics is provided in the Supplementary materials (Table S2).

	Depth (cm)	Porosity[a]	Organic C[b] (wt%)	Clay content (wt%)	$CaCO_3$ (solid) (wt%)	Total S[a] (g kg^{-1})	Total Fe[a] (g kg^{-1})	Total Cu[a] (ppm)
F80 1[c]	1.5–4	0.98	15.5	13	3	22	37	259
F80 2	22–24	0.94	2.8	20	4	17	54	47
F80 3	40–44	0.91	2.6	22	2	8.8	48	42
Phoxy 1	2–4	0.89	2.1	6	71	1.4	10	47
Phoxy 2	10–12	0.87	2	8	66	8	21	55
Phoxy 3	20–24	0.86	2.4	10	57	7.6	17	45
Strömmen 1	1.5–3	0.95	7.9	18	2	27	56	231
Strömmen 2	20–24	0.92	5.8	20	3	20	49	271
Strömmen 3	32–36	0.96	7.4	17	3	42	64	316

[a] Corrected for salt in the pore water.
[b] Corrected for decalcification and salt in the pore water.
[c] Cu mobilisation investigations using F80 1 were discontinued as a result of the high organic C content, which led to difficulties when filtering samples.

to the beamline in a liquid nitrogen bath before being rapidly transferred into the liquid He cryostat. The energy was calibrated during each sample scan by setting the first *K*-edge inflection point of a simultaneously measured Cu foil to 8979 eV (double transmission mode). For each sample, 14 to 15 scans were recorded, depending on the concentration and speciation of Cu. No beam damage was detected. All spectra were averaged and normalized using the ATHENA software (Ravel and Newville, 2005). Radial distribution functions around the Cu absorber were obtained by Fast-Fourier-transformation of the k^3-weighted experimental v(k) function using a Kaiser- Bessel apodization window with the Bessel weight fixed at 2.5. Then, Cu *K*-edge EXAFS data were analysed by linear combination-least squares (LC-LS) fitting procedure using the ATHENA software. Linear coefficients were only constrained to be positive. The accuracy of this fitting procedure ranges between ±25 % and ±5 % of the stated values for each individual contribution and the detection limit for minor species is estimated to be ~10 % (Cancès et al., 2005; Ostergren et al., 1999). Simultaneously, Cu *K*-edge EXAFS data were also analysed by shell-by-shell fitting using the program ARTEMIS and the feff8 code 8.4 (Ankudinov et al., 1998). Backscattering phase and amplitude functions were calculated using the feff8 program for Cu—C, Cu—O, Cu—S, Cu—Cu, and Cu—Fe pairs, based upon CIF files from the Inorganic Crystal Structure Database (ICSD-1517, Version 5.0.0, Data Release 2023.1) (Zagorac et al., 2019) of $CuCO_3$ (Seidel et al., 1974), $CuFeS_2$ (Hall and Stewart, 1973), CuS (Takéuchi et al., 1985), and CuS_2 (Cava et al., 1981). Fits were performed in R-space over a 1.1–4.5 Å range, and all paths were single scattering. Only interatomic distances with acceptable uncertainty values were used in the final fit. The quality of the LC-LS and shell-by-shell fits was estimated by an R-factor parameter (Rf) of the following form: $Rf = \Sigma(k^3\chi_{exp} - k^3\chi_{fit})^2 / \Sigma(k^3\chi_{exp})^2$.

A large set of experimental Cu *K*-edge XAS spectra from natural and synthetic model compounds was used for visual comparison of spectral similarities and for the LC-LS fitting analysis of the EXAFS spectra (EXAFS spectra of LC-LS fits are reported in Fig. S1). Our Cu *K*-edge model compounds dataset includes experimental data already collected and described for a large variety of Cu compounds (Table S4; Tella et al., 2016). In addition, our dataset also includes Cu *K*-edge XAS data for Cu-bearing montmorillonite and kaolinite. The XAS spectra of reference compounds were collected under the same conditions as the XAS spectra of the sediment samples described in this study. For Cu-bearing montmorillonite and kaolinite, the measured reference spectra were compared to spectra reported by Brigatti et al. (2004) and Sonoda et al. (2019), respectively. The model compounds used for the LC-LS fitting analysis are reported in Fig. S2.

2.5. Copper mobilisation experiments

Cu mobilisation from marine sediments in the presence of mb was investigated in kinetic batch experiments under anoxic conditions in a N_2-filled glovebox. 0.1 g aliquots of sediment were pre-equilibrated in 4.5 mL SOW for 3 days in the presence of 200 mg L^{-1} Bronopol (2-bromo-2-nitro-1,3-propanediol) to suppress microbial activity and prevent mb degradation during experiments. The final sediment-to-solution ratio (SSR) of 20 g L^{-1} lies within one order of magnitude of the original SSR of the surface sediments (130–400 g L^{-1}) used in this study. The solution pH was buffered between pH 6.7–7.9 (Table 2) by carbonates in the sediment and SOW.

After pre-equilibration, 0.5 mL of a 0.2 mM mb stock solution was added to 4.5 mL sediment suspensions ($t = 0$; final mb concentration: 20 μM). To examine the effect of mb concentration on Cu mobilisation, select sediments (Phoxy 2 and Strömmen 2) were additionally treated with higher dose of 60 and 140 μM mb. Also, controls without mb were prepared by adding 0.5 mL UPW. The duplicate reactors were shaken continuously on an end-over-end shaker in the dark (to avoid photodegradation of mb). Solution pH was monitored during the experiment. Samples were taken for up to 16 days at regular intervals (0.25, 1, 4, 8, 24, 48, 96, 192, and 384 h for sediments from the F80 and Phoxy stations, and 0.083, 0.25, 0.5, 1, 2, 4, 8, 24, 384 h for sediments from

Table 2
Overview of parameters from the Cu mobilisation experiments. Total Cu per reactor is expressed as the equivalent dissolved Cu concentration in 20 g L^{-1} sediment suspensions. Dissolved Cu concentration is the final mobilised Cu concentration at $t = 384$ h in presence of 20 μM mb (Fig. 2); based on these concentrations, the proportion of Cu mobilised was calculated. The pH hardly changed during the experiments; therefore, an average is presented for duplicate reactors over time.

Sediment	Total Cu per reactor (μM)	Dissolved Cu (μM) (384 h) in presence of 20 μM mb	Proportion Cu mobilised (%)	pH (±0.3)
F80 2	14.8	0.6	4.1	7.79
F80 3	13.2	0.4	3.0	7.75
Phoxy 1	13.0	5.7	44.0	7.20
Phoxy 2	17.4	6.7	38.6	7.28
Phoxy 3	14.2	5.8	40.9	7.38
Strömmen 1	72.6	0.5	0.7	7.28
Strömmen 2	85.4	5.1	6.0	7.29
Strömmen 3	99.5	5.7	5.7	6.72

Strömmen). Samples were centrifuged at 5000 rpm for 30 s, the supernatant was filtered (0.22 μm polyvinylidene fluoride filters (PVDF) Millex-GV), and the filtrate was acidified (1 % HNO_3). Samples involving sediment F80 1 were difficult to filter, possibly due to the high clay or C_{org} content (Table 1). Therefore, experiments with F80 1 were discontinued.

2.6. Methanobactin adsorption experiments

Adsorption isotherms for free mb ligand and mb complexing Cu to F80 2, Phoxy 2, Strömmen 1 and 2 were determined. A Cu-mb stock with a 1:1 Cu-to-mb ratio was prepared at least 10 min before the start of the experiment to allow all Cu to be complexed by mb, as previously established (El Ghazouani et al., 2011). Batch sediment suspensions (20 g L^{-1}) were then treated with the free mb ligand or the Cu-mb complex to final concentrations of 5, 10, 20 or 40 μM. Samples were collected after 15 min of interaction, centrifuged and filtered (0.22 μm cellulose acetate filters) for analysis by UV–vis spectrometry (Cecil CE 1011). This short interaction time was chosen to minimize the effect of metal complexation on the isotherms of free mb. The total concentration of mb remaining in solution was determined at 423 nm, the isosbestic point of the spectra of free mb and Cu-mb complexes. Note that this wavelength differs slightly from the previously reported 422 nm (Pesch et al., 2012), possibly because these adsorption experiments were conducted in SOW with a higher ionic strength. The adsorbed mb concentration was calculated as the difference between the added concentration and the concentration in the filtrate. As light absorbance was measured at the isosbestic point for Cu-mb and mb, the concentration measurements were independent of the speciation of mb in the filtrate.

2.7. Solute concentration measurements by ICP-OES and ICP-MS

Total concentrations of dissolved metals and sulphur in filtered samples from time series experiments and in extracts from the sequential extraction procedure were determined using inductively coupled plasma optical emission spectrometry (ICP-OES) (Perkin-Elmer models Optima 5300-DV and Avio 500). ICP-OES had a limit of quantification (LOQ) of 0.001–0.026 ppm, depending on the element, and a recovery of 100 % ± 5 %. In cases where metal contents in the sediment were low, we additionally used inductively coupled plasma mass spectrometry (ICP-MS) (models Agilent-7700 and Perkin-Elmer NexION2000) to measure metal concentrations in the extracts. ICP-MS analysis had a LOQ of 0.04–8 ppb (except Hg which had an LOQ of 40 ppb), depending on the element, and a recovery of 100 % ± 5 %. Solution pH was monitored using an Orion 3-star pH meter (Thermo).

3. Results

3.1. Sediment characterization

3.1.1. General sediment properties and total contents

The pH of all sediment suspensions was between 7.2 and 7.8, except for Strömmen 3 (pH 6.72). (Table 2), corresponding with the circumneutral pH typically observed in marine sediment porewaters (Silburn et al., 2017). A summary of sediment properties is presented in Table 1. The table combines the sediment characterization performed in the context of this and previous studies investigating the same set of sediment samples. Total contents of potentially competing elements in the sediments were also quantified (Table S2). In these sediments, the organic C content ranged from 2 to 15.5 wt%, the clay content from 6 to 20 wt%, the $CaCO_3$ content from 2 to 71 wt%, the total S content from 1.4 to 42 g kg^{-1}, and the total Fe content ranged from 9.8 to 64 g kg^{-1}. Results on solid phase Fe and S speciation from sequential extractions are presented in Fig. S3 (including the accompanying text) and Table S5.

3.1.2. Solid phase distribution of Cu using sequential extraction

Total Cu content and Cu species distribution in the solid phase were investigated to elucidate the effect of Cu speciation on Cu mobilisation by mb (Fig. S3a and Table S5). Total Cu contents across the different sediment samples varied within one order of magnitude (Table 1), and were measured at <1 μmol g^{-1} Cu (45–55 mg kg^{-1}) in all Phoxy sediment layers, 0.7–4.1 μmol Cu g^{-1} (42–260 mg kg^{-1}) in F80 sediment layers (highest content in the uppermost layer), and 3.6–5.0 μmol Cu g^{-1} (230–320 mg kg^{-1}) in the Strömmen sediment layers (increasing with depth). The results from the sequential Cu extraction demonstrated distinct differences in Cu speciation among the sediments. *Exchangeable Cu* was generally below the LOQ for ICP-MS (3.2 ppb), except for Strömmen 2 and 3, and so was Cu in the *Reducible* fraction, except for Phoxy 1 and Strömmen 3 (Table S5). Contrary to the other sediments, Cu was not measurably extracted in the *Acid-soluble* fraction of the F80 sediments and Strömmen 1. In the F80 sediments, Cu was only present in the *Organic + Cu sulphide* and the *Residual* fraction, the *Residual* Cu content being consistently larger. Although the *Organic + Cu sulphide* fraction represented the highest proportion of Cu at all three Phoxy sediments, the distribution of Cu in the shallower sediment Phoxy 1 differed from the sediments Phoxy 2 and 3, (Fig. S3a). Phoxy 1 had a comparatively large proportion of Cu attributed to the *Acid soluble*, *Reducible* and *Organic + Cu-sulphide* fractions, and, contrary to Phoxy 2 and 3, no measurable Cu in the *Residual* fraction. Strömmen 1, the shallowest Strömmen sediment, differed from Strömmen 2 and 3 by having all Cu attributed to only the *Organic + Cu sulphide* and *Residual* fractions, with *Organic + Cu sulphide* being largest proportion. Strömmen 2 and 3 also had similar Cu distributions with additional *Exchangeable*, *Acid soluble* and *Reducible* fractions, with the *Residual* fraction being the largest proportion (Fig. S3a). Strömmen 3, however, had higher proportions of Cu associated with the *Exchangeable*, *Acid soluble* and *Reducible* fractions than Strömmen 2.

3.1.3. Solid phase Cu speciation analysis by X-ray absorption spectroscopy

The Cu *K*-edge EXAFS spectra, their corresponding Fourier transforms and shell-by shell fits of the selected bulk sediment samples, Strömmen 1 and 2, Phoxy 2, and F80 2, and select reference compounds, CuS, $CuFeS_2$ and Cu_2S are presented in Fig. 1. EXAFS spectra along with LC-LS fitting curves for the same samples are presented in Fig. S1. The EXAFS spectra of the Strömmen 2 and Phoxy 2 sediments show distinctly different features compared to the F80 2 and Strömmen 1 sediments. These differences are specifically apparent in the corresponding Fourier transforms, which show a different position and shape for the second-neighbor peaks (Fig. 1). While all samples clearly show a dominant Cu − S pair correlation at 1.78–1.82 Å (uncorrected for phase shift), characteristic of Cu sulphides (Fig. 1), Strömmen 2 and Phoxy 2 also show the occurrence of second neighbor peaks at 3.36–3.38 Å (uncorrected for phase shift), characteristic of mono-copper-sulphide, *i.e.*, $CuFeS_2$ and CuS (Fig. 1). Conversely, the Fourier Transforms of Cu *K*-edge EXAFS of F80 2 and Strömmen 1 samples compared well with the Cu_2S model reference spectrum (Fig. 1).

These qualitative observations are corroborated by the shell-by-shell fitting analysis of the Cu—K edge EXAFS data (Fig. 1 and Table 3). Shell-by-shell fitting analysis confirms that Strömmen 2 and Phoxy 2 samples exhibit Cu—S, Cu—Cu, and Cu—Fe distances in good agreement with the range of distances reported for the structures of CuS, $CuFeS_2$, and Cu_2S. Conversely, Strömmen 1 and F80 2 samples exhibit, predominantly, Cu—S and Cu—Cu distances in good agreement with the range of distances reported for the structure of Cu_2S. Furthermore, the LC-LS fitting analysis of the Cu—K edge EXAFS data confirms that Cu is mainly present in all sediment samples as Cu sulphides (71–100 %) (Table S6 and Fig. S1) and corroborates the shell-by-shell fitting results, suggesting that Cu in Strömmen 2 and Phoxy 2 samples is incorporated in CuS (17 and 15 %, respectively), $CuFeS_2$ (28 and 23 %, respectively), and Cu_2S (45 and 33 %, respectively), while Cu in Strömmen 1 and F80 2 samples is incorporated mainly in Cu_2S (86 and 80 %, respectively).

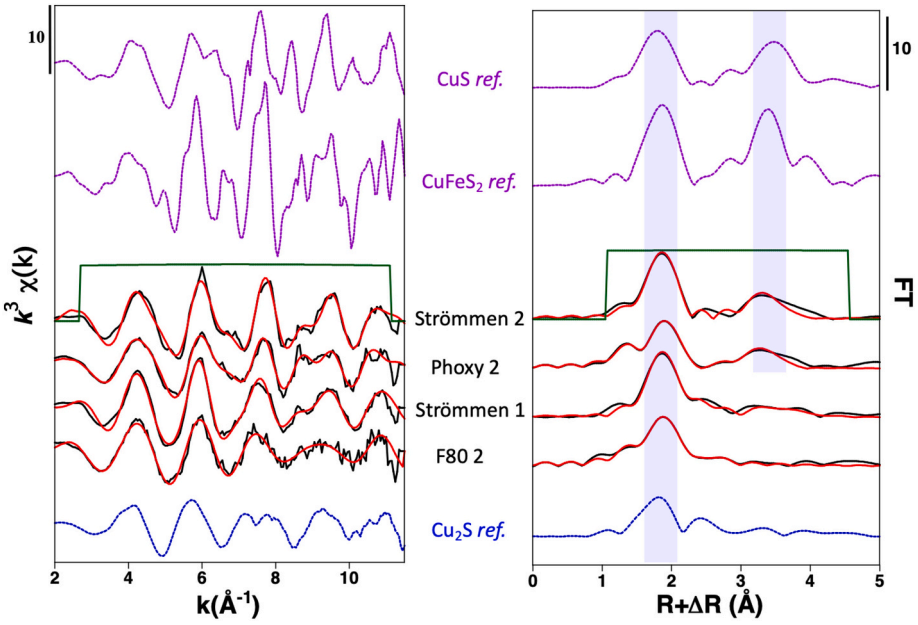

Fig. 1. Shell-by-shell fits of Cu *K*-edge EXAFS spectra of Strömmen 2, Phoxy 2, Strömmen 1, and F80 2 (left). Fitting range $R = 1.1–4.5$ Å, Fourier transform range: k = 2.8–11 $Å^{-1}$ (right). CuS, $CuFeS_2$ and Cu_2S references are displayed above and below for comparison. Purple shading shows the location of two pair correlation characteristic of mono-copper-sulphide, *i.e.*, $CuFeS_2$ and CuS, which are also found in the Fourier transform of Strömmen 2 and Phoxy 2 samples.

In addition to the Cu incorporated in Cu sulphides, shell-by-shell fitting analysis of the Phoxy 2 sample exhibits a Cu—O distance in good agreement with the range of distances reported for the structure of Cu-CO_3 (Behrendt et al., 2022). Using the Cu—C distance (theoretically at 2.48 Å) of Cu-CO_3 in Phoxy 2 did not improve the fit, likely because the Cu—C distance is hidden, or "masked", by the contribution from the Cu—Cu distance (2.41 Å) of Cu_2S. However, addition of Cu-CO_3 in the LC-LS fitting analysis did improve the Rf by 29 % for the Phoxy 2 sample (Table S6). Consequently, the Cu-CO_3 reference compound was systematically included in the LC-LS fitting analysis of all samples to allow for direct comparison of all EXAFS spectra. Based on this analysis, the remaining fraction of Cu is not incorporated in Cu-sulphide phases but associated with Cu carbonates (with 10, 29 and 10 % for Strömmen 2, Phoxy 2, and F80 2, respectively).

3.2. Cu mobilisation from marine sediments

Cu mobilisation from F80, Phoxy and Strömmen sediments was investigated in the presence and absence of mb under anoxic conditions (Fig. 2). In the absence of mb, mobilised Cu concentrations remained <2 µM in all sediment suspensions for the duration of the experiment. For the Strömmen sediments, without addition of mb, dissolved Cu concentrations differed notably between the three depths (Fig. 2c). They were <0.5 µM for Strömmen 1, while for the deeper sediments, Strömmen 2 and 3, the highest concentrations observed were 1 µM and 1.8 µM, respectively.

The effect of mb on Cu mobilisation differed among the tested sediments (Fig. 2 and Table 2). Addition of 20 µM mb had no discernible effect on Cu mobilisation from F80 sediments (Fig. 2a), whereas it led to increased dissolved Cu concentrations in Phoxy and Strömmen sediment suspensions (Fig. 2b and c). The mobilised Cu concentrations in mb-amended (20 µM) sediment suspensions of Phoxy 1, 2 and 3 were similar. After an initial increase within the first 96 h, Cu concentrations remained relatively constant (5.6–6.7 µM) throughout the experimental period (Fig. 2b). Interestingly, the addition of mb increased dissolved Cu concentrations much more for the deeper Strömmen 2 and 3 (up to 6.3 µM) than for the shallower sediment Strömmen 1 (up to 0.5 µM), compared to the respective controls (Fig. 2c). Cu was mobilised much faster in Strömmen 2 and 3 sediments than in Phoxy sediments with a strong increase of soluble Cu concentrations within 2 h in Strömmen 2 and 3 sediments (Fig. 2c). Then, after reaching maxima of 6.4 and 7.8 µM Cu at 24 h, dissolved Cu concentrations decreased to 5.1 and 5.7 µM after 384 h in Strömmen 2 and 3, respectively (Fig. 2c).

Total Cu per reactor varied among sediment suspensions (Table 2; expressed as equivalent solution concentration). Strömmen sediment suspensions had the highest total Cu concentrations (72.6–99.5 µM), 4–8 times higher than F80 and Phoxy sediments (13–17 µM). Variation in total Cu concentrations among samples from different depths at the same station (*i.e.*, same sediment core) was comparatively low (<30 %). The percentage of total Cu mobilised in presence of mb was calculated based on the dissolved Cu concentration in presence of mb after 384 h (Table 2). While only 3–4 % of the total Cu in F80 suspensions was mobilised in presence of mb, ~40 % was mobilised in Phoxy suspensions. <1 % of the total Cu in Strömmen 1 was mobilised in presence of mb, in contrast to ~6 % in Strömmen 2 and 3.

Cu mobilisation from Phoxy 2 and Strömmen 2 sediments was further examined in presence of 60 and 140 µM mb (Fig. 3). For Phoxy 2, for the first 96 h, Cu mobilisation rates did not seem to be affected by the amount of mb applied (Fig. 3a). Between 96 and 384 h, the rate of Cu mobilisation was somewhat larger in incubations with higher mb concentrations, but differences in total mobilised Cu concentrations remained relatively small (6.7 to 8.7 µM after 384 h) (Fig. 3a). For Strömmen 2, the Cu mobilisation rates were also comparable for the various applied mb concentrations in the very initial phase (<5 h). Compared to Phoxy 2, the amount of applied mb had a much larger effect on the mobilised Cu concentration after 384 h, with final Cu concentrations of 23 µM and 36 µM in presence of 60 µM and 140 µM mb, respectively (Fig. 3b). Thus, whereas, at 20 µM mb, the final mobilised Cu concentrations were in the same order of magnitude for Strömmen 2 (5.1 µM) and for Phoxy 2 (6.7 µM), upon application of higher mb concentrations, the final mobilised Cu concentrations were much higher for Strömmen 2 (up to 36 µM) than for Phoxy 2 (up to 8.7 µM). In contrast to Phoxy 2, the final dissolved Cu concentrations mobilised from Strömmen 2 (*i.e.*, after 384 h), were directly proportional to the applied mb concentration (Fig. 3c).

Table 3
Results of shell-by-shell fitting of Cu *K*-edge EXAFS spectra of Strömmen 2, Phoxy 2, Strömmen 1, and F80 2. Corresponding experimental and calculated curves are plotted in Fig. 1. Single scattering paths of $CuFeS_2$, CuS, and Cu_2S references calculated by feff code 8.4 are displayed below for comparison with samples. Calculations are based on crystallographic data from Hall and Stewart (1973) for $CuFeS_2$, Takéuchi et al. (1985) for CuS, and Cava et al. (1981) for CuS_2.

Sample	Path	R (Å)[a]	CN[b]	σ^2 (Å^2)[c]	ΔE_0 (eV)[d]	Rf[e]
Strömmen 2	Cu-S	2.28 ± 0.02	3.55 ± 0.69	0.006 ± 0.002	4.144	0.0293
	Cu-Cu	2.27 ± 0.02	8.49 ± 4.9	0.014 ± 0.004	–	–
	Cu-Cu	3.43 ± 0.02	1*	0.014 ± 0.004	–	–
Phoxy 2	Cu-O	1.88 ± 0.02	1.14 ± 0.25	0.004 ± 0.002	0.402	0.0137
	Cu-S	2.27 ± 0.02	1.82 ± 0.45	0.004 ± 0.002	–	–
	Cu-Cu	3.41 ± 0.02	1*	0.010 ± 0.003	–	–
	Cu-Fe	3.70 ± 0.02	4.26 ± 2.43	0.010 ± 0.003	–	–
F80 2	Cu-S	2.11 ± 0.04	1.05 ± 0.19	0.003*	−2.797	0.0063
	Cu-S	2.30 ± 0.03	3.20 ± 0.71	0.004 ± 0.002	–	–
	Cu-Cu	2.63 ± 0.03	0.35 ± 0.31	0.004 ± 0.002	–	–
	Cu-Cu	2.66 ± 0.03	0.35 ± 0.31	0.004 ± 0.002	–	–
	Cu-Cu	2.71 ± 0.03	0.35 ± 0.31	0.004 ± 0.002	–	–
Strömmen 1	Cu-S	2.31 ± 0.02	3*	0.005 ± 0.002	2.747	0.0161
	Cu-Cu	2.66 ± 0.03	1*	0.007 ± 0.004	–	–
	Cu-Cu	2.69 ± 0.03	1*	0.007 ± 0.004	–	–
	Cu-Cu	2.74 ± 0.03	1*	0.007 ± 0.004	–	–
	Cu-Cu	2.87 ± 0.03	2*	0.007 ± 0.004	–	–
	Cu-Cu	3.00 ± 0.03	1*	0.010 ± 0.003	–	–
	Cu-Cu	3.10 ± 0.03	1*	0.010 ± 0.003	–	–
	Cu-Cu	3.38 ± 0.03	1*	0.010 ± 0.003	–	–
	Cu-S	3.90 ± 0.08	4*	0.017 ± 0.011	–	–
	Cu-Cu	4.12 ± 0.09	2*	0.010 ± 0.013	–	–

Single scattering calculated by feff8.4 for a cluster size of 5 Å

Reference	Path	R (Å)	CN
$CuFeS_2$	Cu-S	2.3	4
	Cu-Fe	3.73	8
	Cu-Cu	3.71	4
CuS	Cu-S	2.18	3
	Cu-Cu	3.14	6
	Cu-S	3.7	6
	Cu-Cu	3.77	6
Cu_2S	Cu-S	2.31	2
	Cu-S	2.36	1
	Cu-Cu	2.66	1
	Cu-Cu	2.69	1
	Cu-Cu	2.74	1
	Cu-Cu	2.86	2
	Cu-Cu	2.93	1
	Cu-Cu	3.03	1
	Cu-Cu	3.31	1

(–) All parameter values indicated by (–) were linked to the parameter value placed above in the table.
[a] R, the interatomic distance between the absorbing atom and the neighboring shell.
[b] CN, coordination number - the number of atom neighbors in the shell.
[c] σ, the Debye-Waller factor of Cu—O, Cu—S, Cu—Cu, and Cu—Fe.
[d] ΔE_0, the threshold energy correction.
[e] Fit quality was estimated using an R-factor, $Rf = \Sigma(k^3\chi_{exp}-k^3\chi_{fit})^2/\Sigma(k^3\chi_{exp})^2$.
[*] The coordination numbers were fixed to these values.

3.3. Mobilisation of Fe and other metals from marine sediments

Dissolved concentrations of elements that have the potential to compete with Cu for complexation by mb, and possibly impact Cu mobilisation, were also measured (Table S7 and Fig. S4). Mobilised concentrations of Ag, Hg, Co and Ni were <1 μM, even in the presence of mb. Mobilisation of Fe, the most abundant metal in the sediments that could potentially compete with Cu for complexation by mb, did occur in some cases (Fig. S4). For sediments from which Cu was mobilised (Phoxy 1–3, Strömmen 2 and 3), total Fe concentrations in the filtered samples were low (<5 μM) in both the absence and presence of 20 μM mb (Fig. S4b and c), suggesting that mb addition did not affect the dissolved Fe concentration. Much higher Fe concentrations (>100 μM) were observed in filtered samples from suspensions where little Cu was mobilised, even in presence of mb (F80 2 and 3 and Strömmen 1) (Fig. S4a and c). Dissolved Fe concentrations were initially high but declined during the experiment by ~85–90 % in the F80 suspensions, and by ~70 % in the Strömmen suspensions. In select samples from F80 suspensions, dissolved Fe was present mostly (>82.5 %) as Fe(II), as determined *via* the Ferrozine method (Viollier et al., 2000) (Table S8). Because of the poor solubility of Fe(III) minerals at the circumneutral pH of the sediment suspensions, dissolved Fe(III) concentrations are also presumed to be low in other sediment suspensions in which Fe was mobilised. Sediments from which Fe was mobilised generally had higher Fe contents attributed to the HCl-Fe(II) fraction (215–406 μmol g^{-1}) than sediments from which Fe was hardly mobilised (9–233 μmol g^{-1}) (Fig. S3b and Table S5), suggesting surface-sorbed Fe(II).

In corresponding treatments with and without mb addition, Fe concentrations initially differed by up to 13 % for all sediments. In F80 suspensions dissolved Fe concentrations were higher in the treatments

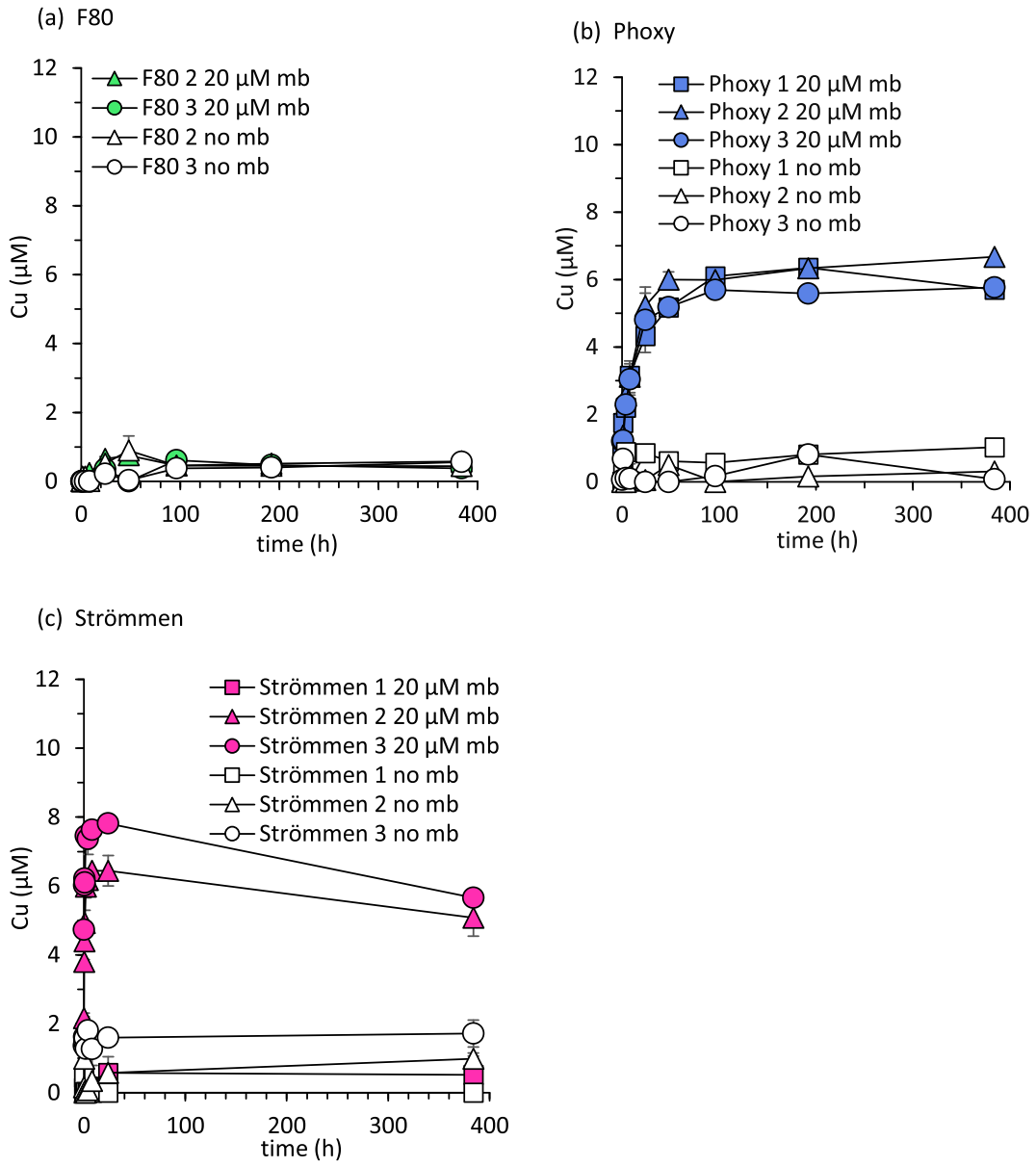

Fig. 2. Cu mobilisation from F80 (a), Phoxy (b), and Strömmen (c) sediments (20 g L^{-1} in SOW + 0.2 g L^{-1} Bronopol) in the presence of 20 µM mb (filled symbols) and absence of mb (open symbols) under anoxic conditions. The numbers 1–3 represent different sediment layers. Error bars indicate standard deviations of duplicate reactors.

without mb for the first 8 h (Fig. S4a), whereas in Strömmen 1 they were higher in the treatment with mb - by 45 µM, exceeding the applied mb concentration (20 µM) more than twofold (Fig. S4c). During the experiment, the Fe concentrations in corresponding treatments with and without mb converged (Fig. S4a and c). Dissolved Fe concentrations mobilised from Phoxy 2 and Strömmen 2 did not increase with increasing mb concentration and remained low (<7 µM), even when the mb concentration was increased to 140 µM (Fig. S5a and b).

3.4. *Methanobactin adsorption to marine sediments*

Adsorption of free mb ligand and of mb in complexes with Cu (Cu-mb) to various sediments was examined to assess the potential fraction of applied ligands adsorbing to the sediments. Through our spectrophotometric method, the total mb concentrations remaining in solution were analysed; adsorption results for mb complexing Cu are interpreted in terms of *total adsorbed* and *solution* concentrations of mb, and not for a Cu-mb complex of a specific stoichiometry (see SI section 'Methanobactin speciation and adsorption to marine sediments' and Fig. S6).

The adsorption data were fit to a linear adsorption isotherm equation: $Q = \alpha \cdot C$; where Q (µmol kg^{-1}) is the total adsorbed mb ligand content (either free or as a complex), α (L kg^{-1}) the adsorption coefficient, a measure for the affinity of the ligand/complex for the solid phase, and C (µmol L^{-1}) the total solution concentration of the mb ligand (Fig. 4 and Table 4). As only the total dissolved mb ligand concentrations were measured, changes in solution speciation due to metal complexation, displacement and dissociation reactions could not be accounted for. Nonetheless, results from the adsorption experiments still allow us to estimate the overall partitioning of the mb ligand over the solid and solution phase in Phoxy 2 and Strömmen 2 sediment suspensions.

For all sediments, less mb remained in solution when applied as free mb ligand (α = 8.4–23.2 L kg^{-1}) compared to 1:1 Cu-mb complex (α = 4.7–11.8 L kg^{-1}). This suggests that the free ligand has a larger affinity for the solid phase than mb complexing Cu. The difference in mb

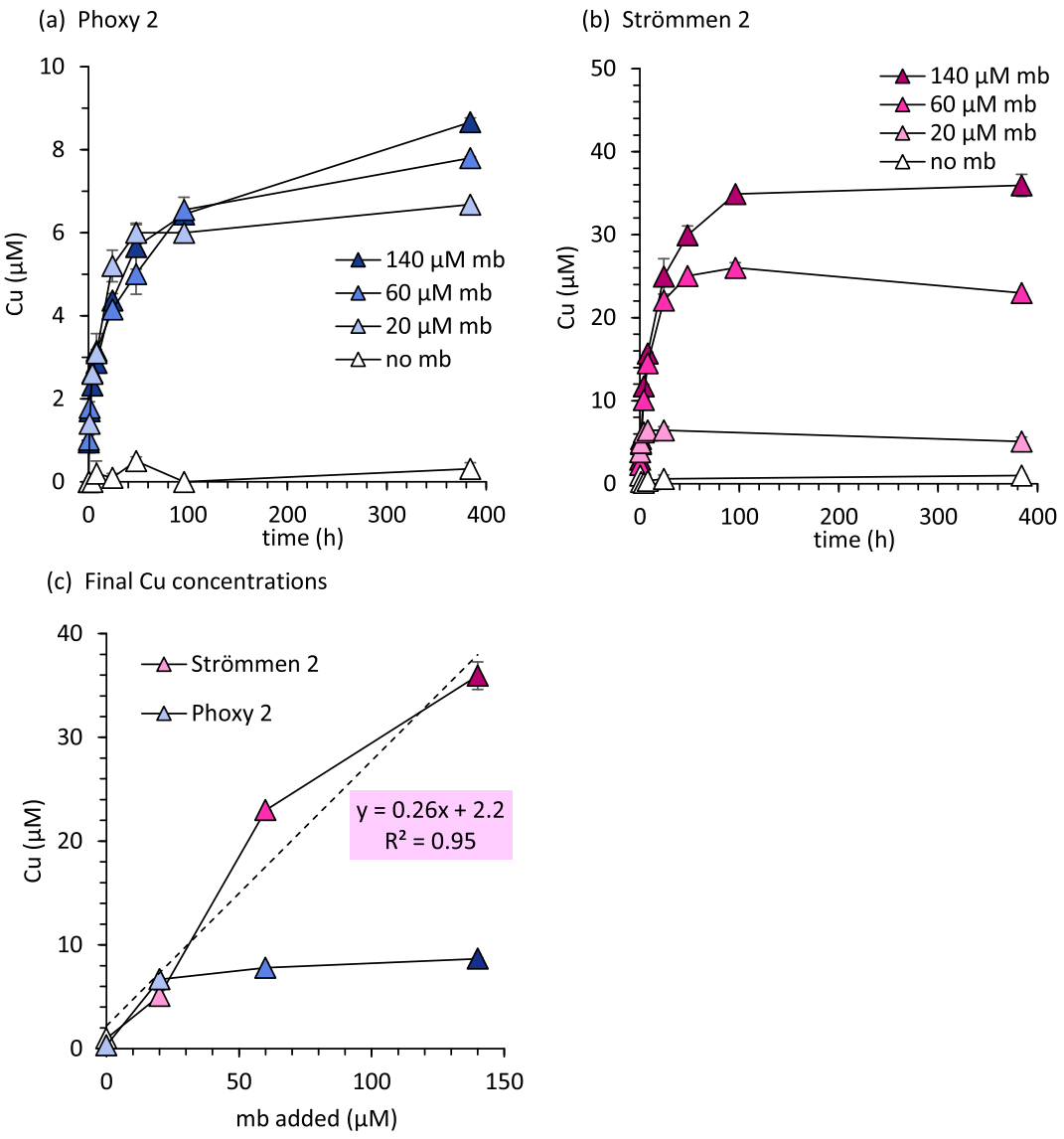

Fig. 3. Cu mobilisation from Phoxy 2 (a) and Strömmen 2 (b) sediments (20 g L^{-1} in SOW + 0.2 g L^{-1} Bronopol) in the presence of 20, 60 and 140 µM mb (filled symbols) and absence of mb (open symbols) under anoxic conditions. Final Cu concentrations (after 384 h) mobilised from Strömmen 2 (pink) and Phoxy 2 (blue) are also plotted against added mb concentration (c). Error bars indicate standard deviations of duplicate reactors.

adsorption between free mb- and Cu-mb treatments was largest for sediments from which little Cu was mobilised (F80 2 and Strömmen 1; Fig. 2), up to a factor 4.7 based on the α values. For Phoxy 2, the adsorption coefficients for the two treatments were almost the same and also, for Strömmen 2, the difference was relatively small (~35 %) (Fig. 4 and Table 4). The smaller differences between the two treatments for Phoxy 2 and Strömmen 2 can, in part, be explained by the formation of Cu-mb complexes during the timespan of the adsorption test.

4. Discussion

4.1. Solid phase Cu speciation influences Cu mobilisation by mb

Dissolved Cu concentrations increased in the presence of mb in some sediment suspensions, but not in all (Fig. 2), even though each reactor contained at least 13 µM Cu (on a solution concentration basis) (Table 2), which would suffice to form 1:1 Cu-mb complexes with over half of the added mb (20 µM). Furthermore, total Cu content does not predict the extent of Cu mobilisation from these sediments. Instead, different extents of Cu mobilisation by mb are likely controlled by differences in solid-phase Cu speciation. It has been demonstrated that mb can mobilise Cu from NOM constituents (Pesch et al., 2013) and from several Cu-bearing mineral phases, including Cu oxides, malachite ($Cu_2CO_3(OH)_2$) (Fru et al., 2011), borosilicate glass (Kulczycki et al., 2007) and Cu sulphides (Rushworth et al., 2022) in model systems. However, the geochemical conditions (including pH and redox potential) and mineral phases present in marine sediments may promote or inhibit Cu mobilisation by mb.

XAS showed a clear distinction in Cu mineral phases between sediments and Cu was only mobilised from sediments that contained a mono-Cu-mono-sulphide (CuS) phase (Phoxy 2 and Strömmen 2) (Table 3). Other Cu sulphide minerals were present in all sediments, but CuS was only identified in sediments where Cu was mobilised, suggesting that CuS likely played a critical role in Cu mobilisation by mb. The amount of Cu attributed to CuS in sediments (based on the values reported for the LC-LS fits – Table S6) could account for 30 % (Phoxy 2) and 38 % (Strömmen 2) of the maximum Cu concentrations mobilised in the presence of 140 µM mb (Table S9). Rushworth et al. (2022) demonstrated that the efficacy of mb at mobilising Cu from mono-Cu-sulphide minerals is phase dependent. They observed that under

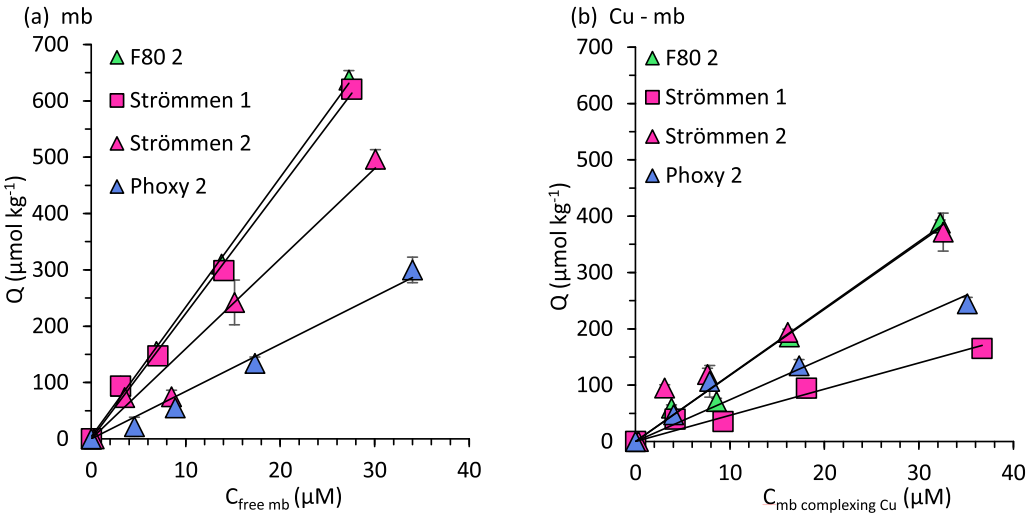

Fig. 4. Adsorption isotherms for mb when applied as (a) metal-free mb ligands and (b) 1:1 Cu-mb complexes to select sediments (20 g L^{-1}) in SOW. The corresponding equations are presented in Table 4.

Table 4
Fits to linear adsorption isotherms for adsorption data of mb applied as free mb ligand and 1:1 Cu-mb complexes to various sediments, where Q (µmol kg^{-1}) is the total adsorbed mb ligand content (either free or as a complex), C is the solution concentration (µM), and Ads-% is the percentage of mb adsorbed at a solid to solution ratio (SSR) of 20 g L^{-1}.

	Free mb-ligand			mb complexing Cu		
Sediment	Linear fit	R^2	Ads-%	Linear fit	R^2	Ads-%
F80 2	Q = 23.2*C	0.999	31.7	Q = 11.7*C	0.994	19.0
Phoxy 2	Q = 8.4*C	0.991	14.4	Q = 7.4*C	0.968	12.9
Strömmen 1	Q = 22.3*C	0.998	30.8	Q = 4.7*C	0.985	8.5
Strömmen 2	Q = 16.0*C	0.987	24.2	Q = 11.8*C	0.978	19.1

experimental conditions similar to those in our present study (pH 7.5–8.5, anoxic conditions) more Cu was mobilised from CuS than from $CuFeS_2$. There is also evidence that the affinity of mb for Cu may be insufficient to measurably dissolve Cu from certain Cu sulphide phases, which also might explain why Cu was not mobilised from sediments in our experiments. Fru et al. (2011), for example, observed that Cu_2S, which was determined as the dominant Cu sulphide phase in all sediments probed in this study using XAS (Fig. 1 and Table 3), did not dissolve in the presence of mb. The amount of Cu associated with CuS (calculated as the total Cu content multiplied with the fraction determined by XAS; Table S9) in our experiment is, however, too small to account for the total Cu mobilised by mb; for Phoxy 2 this was already the case in the 20 µM mb treatment, for Strömmen 2 this was observed only in the 60 and 140 µM mb treatments. This implies that Cu from other Cu-bearing phases (Table 3) was also mobilised by mb, like another mono-Cu-sulphide phase, $CuFeS_2$. Both CuS and $CuFeS_2$ phases have Cu as Cu(I) in the structure (Boekema et al., 2004), making it more susceptible to oxidation and release (Kumar et al., 2013). However, it is also important to note that Cu was not mobilised from Strömmen 1 where only $CuFeS_2$ was detected at a low content, and no CuS. CuS is often found on the surface of $CuFeS_2$ particles where it can catalyse the oxidation of mixed redox couple phases like $CuFeS_2$ to allow for Cu release (Todd et al., 2003). So, in our experiment with Strömmen 1, the absence of CuS may have inhibited the release of Cu from the $CuFeS_2$ phase. In the 140 µM mb treatments with Phoxy 2 and Strömmen 2 sediments, the mobilised Cu concentration after 384 h scaled, approximately proportionally, with the amount of Cu present as CuS (Table S9). The larger Cu mobilisation rate from Strömmen 2 compared to Phoxy 2 (Figs. 2b & c and 3a & b) may also have been related to the larger quantity of CuS and $CuFeS_2$ in the former, and to differences in the crystallinity of mineral phases; for example, Rushworth et al. (2022) observed faster Cu mobilisation by mb from poorly crystalline Cu sulphides than from more crystalline Cu sulphide phases. In conclusion, our experimental results suggest that the exudation of mb in sulphide-bearing marine sediments can efficiently enhance dissolved Cu concentrations, when mono-Cu-mono-sulphide phases are present.

During sequential extractions, in sediments from which Cu was not mobilised, Cu was only extracted in the Organic + Cu sulphide (F4) and Residual (F5) fractions (representing Cu associated with Cu sulphides, refractory organic material, and silicate minerals or pyrite; Fig. S3a and Table S3). All sediments, from which Cu was mobilised by mb (Fig. 2) contained measurable Cu concentrations in the Acid soluble fraction (F2; Cu bound to carbonates, AVS or labile Cu-OM species; Table S5), but only Strömmen 2 and 3 contained Cu in the Exchangeable fraction (F1 weakly sorbed species), and only Phoxy 1 and 3 contained Cu in the Reducible fraction (F3; Fe and Mn (oxyhydr)oxides and labile metal-organic complexes). Considering all sediments, the amount of Cu extracted in F1–3 accounted for 1–65 % of the amount mobilised by mb (Fig. S3a and Tables S5 and S6). Hence, it appears that the sequential extraction employed here is not a good predictor for Cu availability with regards to mobilisation by mb and we could not clearly elucidate which fraction/solid phase Cu species Cu was mobilised from in the presence of mb. Although Cu was only mobilised by mb from sediments in which Cu was extracted in F2 (Fig. S3a), the amount of Cu extracted in this fraction was lower by a factor of 50–60 compared to the Cu concentrations mobilised by mb (Table S5). The extractant used for F2 (1 M acetic acid/acetate at pH 4.5) is supposed to extract Cu associated with carbonates, AVS and labile Cu-organic complexes. However, incomplete extraction of target phases, as reported by Burton et al. (2006) for AVS, and redistribution of Cu over (remaining) solid phases during the sequential extraction procedure, a phenomenon reported in several other studies (Kheboian and Bauer, 1987; Rendell et al., 1980), may both obscure the solid Cu phases driving Cu mobilisation by mb, suggesting a different solid-phase Cu speciation compared to XAS. See the text associated with Table S3 for a detailed description of proposed differences on what phases may be extracted in each fraction.

Cu complexation by refractory NOM, like humic substances, contributes to the dissolved Cu pool in many marine environments and can play a role in limiting the Cu bioavailability (Ruacho et al., 2022). However, it has been shown that mb can effectively compete with humic substances for binding Cu (Pesch et al., 2013), and that humic substances do not inhibit mb-controlled dissolution of Cu sulphide nanoparticles (Rushworth et al., 2022). Also, our XAS results suggest that Cu

complexation by NOM does not significantly contribute to the solid phase Cu speciation in the sediments used in this experiment. Considering our XAS results on Cu speciation in the sediments, and the findings from previous studies, which show that Cu is easily mobilised by mb in the presence of NOM (Pesch et al., 2013; Rushworth et al., 2022), it is improbable that Cu-NOM complexes constrained Cu mobilisation from the sediments by mb. It seems more likely that the Cu extracted in F4 (organic + Cu sulphide) of the sequential extraction was mostly associated with Cu sulphide minerals.

4.2. Competition from other elements for complexation of mb

Marine sediments contain several trace metals known to form complexes with mb (Choi et al., 2006; McCabe et al., 2017). In this study, however, most of the potentially competing trace metals investigated (Ag, Hg, Ni, Co) were not measurably mobilised by mb (Table S7), and therefore, their presence in the sediment did not inhibit Cu mobilisation. Presumably, this resulted from the lower affinity of mb for these metals compared to Cu (Choi et al., 2006; McCabe et al., 2017), and the low free solution concentrations and total contents of these metals in the sediment (Table S2).

High dissolved Fe(II) concentrations in filtered samples were measured in treatments where little Cu was mobilised, irrespective of the presence or absence of mb (Table S8). However, mb may interact with dissolved Fe in solution forming Fe-mb complexes. Rushworth et al. (2022) observed elevated dissolved Fe concentrations upon addition of mb to oxic suspensions of a natural $CuFeS_2$ sample at circumneutral pH and also demonstrated that mb interacts with Fe(II) but not Fe(III). Under such conditions, in absence of ligands, Fe(II) oxidizes to Fe(III), which subsequently precipitates, but mb could maintain Fe(II) in solution by complexation. Also, Klar et al. (2017) observed dissolved Fe(II) in the vicinity of oxic-anoxic interfaces in porewaters of the Celtic Sea, which they concluded was stabilized by the presence of ligands. Therefore, it cannot be excluded that dissolved Fe(II) affected the rate and extent of Cu mobilisation by mb in this study.

4.3. The effect of mb on dissolved Cu concentrations in marine systems

In order to transfer the results of this study to large scale natural systems, it is important to consider the effect of solid-to-solution ratios (SSR). Specifically, in compacted sediments the SSR is much higher than the SSR in our sediment suspension batch experiments, leading to considerably more adsorption. The percentage of mb adsorbed to sediments (Ads-%) can be estimated using adsorption coefficient α and the SSR (kg L^1) reflecting natural or experimental conditions *via* the following equation:

$$Ads - \% = \left(\frac{\alpha.SSR}{1 + \alpha.SSR}\right).100\% \quad (1)$$

Following the procedure outlined in Walter et al. (2016), we estimated that, for compact marine sediments with adsorption coefficients for mb in the range determined in this study, and a SSR of 4 kg L^{-1} (particle density (ρ_p) = 2.65 kg L^{-1} and (water-filled) porosity (θ) = 0.4), merely 1–5 % of the total mb ligand is present in the pore water, depending on the sediment, and on whether mb is complexing Cu; the rest is sorbed to the solid phase. This suggests that the efficiency of mb-based Cu acquisition within compact sediments may be low. However, since aerobic methanotrophy requires both oxygen and methane, it is likely limited to oxygenated sediments and bottom waters near the sediment-water interface, receiving methane from cold seeps or from methanogenesis below (Boetius and Wenzhöfer, 2013; Tikhonova et al., 2020). Here, the type of sediment environment reflects the nature of the high-porosity sediment samples investigated in this study (θ = 0.86–0.98; Table 1), which were sampled from an "interfacial sediment zone" situated between the overlying water and the deeper, more compact sediments. Assuming an average ρ_p for marine sediments of 2.65 kg L^{-1} (Burdige, 2007) the sediment samples used in our adsorption experiments have SSR values of 0.13–0.4 kg L^{-1}, much lower than those observed in compact sediments. Under such conditions, a substantially smaller fraction of the total mb will adsorb to the sediments, and 20–30 % of the metal free ligand or 25–63 % of the mb complexing Cu remain in the aqueous phase to facilitate Cu acquisition. The higher proportion of mb adsorbed to F80 2 and Strömmen 2, compared to Phoxy 2 and Strömmen 1, in the Cu-mb treatments might be attributed to differences in solid-phase characteristics between sediments (Tables 1 and S2). In a study on adsorption of metal-phytosiderophore complexes, the adsorbed fraction of metal-ligand complexes correlated with the clay content and the clay/organic C ratio of soils (Walter et al., 2016). A similar correlation was not evident for Cu-mb complex adsorption, yet the number of sediment samples used in this study is too limited to do a comparable analysis.

5. Conclusions

This study has demonstrated that the chalkophore methanobactin exuded by methanotrophs as part of a Cu acquisition strategy can mobilise Cu from Cu sulphide-bearing marine sediments. However, as per our hypothesis, mb-facilitated Cu mobilisation under natural conditions depends on the solid phase Cu speciation: Cu was only mobilised from sediments that contained CuS (mono-Cu-mono-sulphide). This suggests that exudation of mb for Cu acquisition by methanotrophs may be rendered inefficient in marine environments where mono-Cu-mono-sulphide phases are not present. Furthermore, the high affinity of the (metal-)free mb ligand and of mb complexing Cu for sediments suggests that the exudation of mb for Cu acquisition may be most relevant at the sediment-water interface, or in overlying waters where the sediment-to-solution ratio is low, and where the presence of oxygen makes aerobic methanotrophic activity possible. Our results show how solid phase Cu speciation can constrain Cu acquisition by aerobic methanotrophs exuding chalkophores, and, as a consequence, MOx. However, solid phase Cu speciation should not be considered the sole predictor for methanotrophic activity, as other environmental factors may also be limiting. Incubation studies with a chalkophore-exuding methanotroph, like *Methylosinus trichosporium* OB3b, and sediments differing in Cu speciation could further elucidate to what extent solid phase Cu speciation affects MO_x in marine sediments.

In conclusion, our experimental results demonstrate that mb-facilitated Cu acquisition from sulphide-bearing marine sediments is possible despite the high stability of Cu sulphide solid phases, but that it is geochemically constrained. Whether exudation of mb is an efficient strategy for Cu acquisition from marine sediments depends strongly on the solid-phase Cu speciation. In marine environments where the solid-phase Cu speciation is unfavorable, mb does not act to mobilise Cu, and MO_x may be limited.

CRediT authorship contribution statement

Danielle D. Rushworth: Writing – original draft, Visualization, Supervision, Methodology, Investigation, Funding acquisition, Formal analysis, Conceptualization. **Walter D.C. Schenkeveld:** Writing – review & editing, Visualization, Supervision, Resources, Methodology, Funding acquisition, Formal analysis, Conceptualization. **Naresh Kumar:** Writing – review & editing, Visualization, Supervision, Methodology, Conceptualization. **Vincent Noël:** Writing – review & editing, Writing – original draft, Investigation, Formal analysis. **Jannes Dewulf:** Writing – review & editing, Investigation, Formal analysis. **Niels A.G.M. van Helmond:** Writing – review & editing, Investigation, Formal analysis. **Caroline P. Slomp:** Writing – review & editing, Resources, Methodology. **Moritz F. Lehmann:** Writing – review & editing, Funding acquisition, Conceptualization. **Stephan M. Kraemer:** Writing – review & editing, Visualization, Supervision, Resources, Methodology, Funding

acquisition, Conceptualization.

Declaration of competing interest

The authors declare that they have no known competing financial interests or personal relationships that could have appeared to influence the work reported in this paper.

Data availability

Data will be made available on request.

Acknowledgement

The authors would like to thank Dr. Simon K.-M.R. Rittmann and Dr. Carolina Reyes for support in *M. trichosporium* cultivation, and Herwig Lentiz, Barbara Reischl and Thom Claessen for technical support. We thank Andreas Maier for assistance with dissolved organic carbon measurements, Helen de Waard and Coen Mulder for assistance with ICP-MS and ICP-OES measurements, and Klaas Nierop for the measurements with the elemental analyser. Finally, the authors would like to thank Emmanuel Doelsch (Cirad, France) for the large set of experimental Cu *K*-edge XAS spectra from natural and synthetic model compounds used in this work.

Funding

This study was supported by the Austrian Science Fund (FWF project number 12256-N29), the Marietta Blau-Grant, Austria's Agency for Education and Internationalisation (OeAD), as well as Swiss National Science Foundation grant SNSF 169951. NAGMvH and CPS were supported by the ERC Synergy grant MARIX (8540088). Additional funding was provided by the SLAC Floodplain Hydro-Biogeochemistry SFA program of the US DOE, Office of Biological and Environmental Research, Earth and Environmental Systems Sciences Division under DOE Contract No. DE-AC02-76SF00515 (data analysis and writing).

Appendix A. Supplementary data

Supplementary data to this article can be found online at https://doi.org/10.1016/j.scitotenv.2024.173046.

References

Aizenshtat, Z., Krein, E.B., Vairavamurthy, M.A., Goldstein, T.P., 1995. Role of sulfur in the transformations of sedimentary organic matter: a mechanistic overview. In: Geochemical Transformations of Sedimentary Sulfur, vol. 612, pp. 16–37.

Ankudinov, A.L., Ravel, B., Rehr, J.J., Conradson, S.D., 1998. Real-space multiple-scattering calculation and interpretation of x-ray-absorption near-edge structure. Phys. Rev. B 58, 7565–7576.

Behrendt, G., Prinz, N., Wolf, A., Baumgarten, L., Gaur, A., Grunwaldt, J.-D., et al., 2022. Substitution of copper by magnesium in malachite: insights into the synthesis and structural effects. Inorg. Chem. 61, 19678–19694.

Boekema, C., Krupski, A.M., Varasteh, M., Parvin, K., van Til, F., van der Woude, F., et al., 2004. Cu and Fe valence states in CuFeS2. J. Magn. Magn. Mater. 272–276, 559–561.

Boetius, A., Wenzhöfer, F., 2013. Seafloor oxygen consumption fuelled by methane from cold seeps. Nat. Geosci. 6, 725–734.

Boetius, A., Ravenschlag, K., Schubert, C.J., Rickert, D., Widdel, F., Gieseke, A., et al., 2000. A marine microbial consortium apparently mediating anaerobic oxidation of methane. Nature 407, 623–626.

Brigatti, M.F., Colonna, S., Malferrari, D., Medici, L., 2004. Characterization of Cu-complexes in smectite with different layer charge location: chemical, thermal and EXAFS studies 1. Geochim. Cosmochim. Acta 68, 781–788 (Associate editor: D. J. Vaughan).

Bruland, K.W., 1980. Oceanographic distributions of cadmium, zinc, nickel, and copper in the North Pacific. Earth Planet. Sci. Lett. 47, 176–198.

Buck, K.N., Bruland, K.W., 2005. Copper speciation in San Francisco Bay: a novel approach using multiple analytical windows. Mar. Chem. 96, 185–198.

Burdige, D.J., 2007. Geochemistry of Marine Sediments. Princeton University Press.

Burton, E.D., Phillips, I.R., Hawker, D.W., 2006. Factors controlling the geochemical partitioning of trace metals in estuarine sediments. Soil Sediment Contam. Int. J. 15, 253–276.

Burton, E.D., Sullivan, L.A., Bush, R.T., Johnston, S.G., Keene, A.F., 2008. A simple and inexpensive chromium-reducible sulfur method for acid-sulfate soils. Appl. Geochem. 23, 2759–2766.

Cancès, B., Juillot, F., Morin, G., Laperche, V., Alvarez, L., Proux, O., et al., 2005. XAS evidence of As(V) association with iron oxyhydroxides in a contaminated soil at a former arsenical pesticide processing plant. Environ. Sci. Technol. 39, 9398–9405.

Cava, R.J., Reidinger, F., Wuensch, B.J., 1981. Mobile ion distribution and anharmonic thermal motion in fast ion conducting Cu2S. Solid State Ionics 5, 501–504.

Choi, D.W., Do, Y.S., Zea, C.J., McEllistrem, M.T., Lee, S.W., Semrau, J.D., et al., 2006. Spectral and thermodynamic properties of Ag(I), Au(III), Cd(II), Co(II), Fe(III), Hg (II), Mn(II), Ni(II), Pb(II), U(IV), and Zn(II) binding by methanobactin from Methylosinus trichosporium OB3b. J. Inorg. Biochem. 100, 2150–2161.

Christl, I., Kretzschmar, R., 2001. Relating ion binding by fulvic and humic acids to chemical composition and molecular size. 1. Proton binding. Environ. Sci. Technol. 35, 2505–2511.

Claff, S.R., Sullivan, L.A., Burton, E.D., Bush, R.T., 2010. A sequential extraction procedure for acid sulfate soils: partitioning of iron. Geoderma 155, 224–230.

Coale, K.H., Bruland, K.W., 1988. Copper complexation in the Northeast Pacific. Limnol. Oceanogr. 33, 1084–1101.

Crocket, J.H., Macdougall, J.D., Harriss, R.C., 1973. Gold, palladium and iridium in marine sediments. Geochim. Cosmochim. Acta 37, 2547–2556.

DiSpirito, A.A., Zahn, J.A., Graham, D.W., Kim, H.J., Larive, C.K., Derrick, T.S., et al., 1998. Copper-binding compounds from Methylosinus trichosporium OB3b. J. Bacteriol. 180, 3606–3613.

Durisch-Kaiser, E., Klauser, L., Wehrli, B., Schubert, C., 2005. Evidence of intense archaeal and bacterial methanotrophic activity in the Black Sea water column. Appl. Environ. Microbiol. 71, 8099–8106.

Egger, M., Kraal, P., Jilbert, T., Sulu-Gambari, F., Sapart, C.J., Röckmann, T., et al., 2016. Anaerobic oxidation of methane alters sediment records of sulfur, iron and phosphorus in the Black Sea. Biogeosciences 13, 5333–5355.

Egger, M., Hagens, M., Sapart, C.J., Dijkstra, N., van Helmond, N.A.G.M., Mogollón, J.M., et al., 2017. Iron oxide reduction in methane-rich deep Baltic Sea sediments. Geochim. Cosmochim. Acta 207, 256–276.

El Ghazouani, A., Baslé, A., Firbank, S.J., Knapp, C.W., Gray, J., Graham, D.W., et al., 2011. Copper-binding properties and structures of methanobactins from Methylosinus trichosporium OB3b. Inorg. Chem. 50, 1378–1391.

Fitch, M.W., Graham, D.W., Arnold, R.G., Agarwal, S.K., Phelps, P., Speitel Jr., G.E., et al., 1993. Phenotypic characterization of copper-resistant mutants of Methylosinus trichosporium OB3b. Appl. Environ. Microbiol. 59, 2771–2776.

Fitzgerald, W.F., Lamborg, C.H., Hammerschmidt, C.R., 2007. Marine biogeochemical cycling of mercury. Chem. Rev. 107, 641–662.

Flemming, C.A., Trevors, J.T., 1989. Copper toxicity and chemistry in the environment: a review. Water Air Soil Pollut. 44, 143–158.

Fru, E.C., Gray, N.D., McCann, C., Baptista, J.D., Christgen, B., Talbot, H.M., et al., 2011. Effects of copper mineralogy and methanobactin on cell growth and sMMO activity in Methylosinus trichosporium OB3b. Biogeosciences 8, 2887–2894.

Hall, S.R., Stewart, J.M., 1973. The crystal structure refinement of chalcopyrite, $CuFeS_2$. Acta Crystallogr. B 29, 579–585.

Hanson, R.S., Hanson, T.E., 1996. Methanotrophic bacteria. Microbiol. Rev. 60, 439–471.

Hartmann, D.L., Klein Tank, A.M.G., Rusticucci, M., 2014. Observations: atmosphere and surface. In: Climate Change 2013 – The Physical Science Basis: Working Group I Contribution to the Fifth Assessment Report of the Intergovernmental Panel on Climate Change. Cambridge University Press, Cambridge, pp. 159–254 (Intergovernmental Panel on Climate C, editor).

Hermans, M., Lenstra, W.K., van Helmond, N.A.G.M., Behrends, T., Egger, M., Séguret, M.J.M., et al., 2019. Impact of natural re-oxygenation on the sediment dynamics of manganese, iron and phosphorus in a euxinic Baltic Sea basin. Geochim. Cosmochim. Acta 246, 174–196.

Hoffmann, K., Bouchet, S., Christl, I., Kaegi, R., Kretzschmar, R., 2020. Effect of NOM on copper sulfide nanoparticle growth, stability, and oxidative dissolution. Environ. Sci. Nano 7, 1163–1178.

Huerta-Diaz, M.A., Morse, J.W., 1992. Pyritization of trace metals in anoxic marine sediments. Geochim. Cosmochim. Acta 56, 2681–2702.

Jokinen, S.A., Jilbert, T., Tiihonen-Filppula, R., Koho, K., 2020. Terrestrial organic matter input drives sedimentary trace metal sequestration in a human-impacted boreal estuary. Sci. Total Environ. 717, 137047.

Kannan, K., Falandysz, J., 1998. Speciation and concentrations of mercury in certain coastal marine sediments. Water Air Soil Pollut. 103, 129–136.

Kheboian, C., Bauer, C.F., 1987. Accuracy of selective extraction procedures for metal speciation in model aquatic sediments. Anal. Chem. 59, 1417–1423.

Kim, H.J., Graham, D.W., DiSpirito, A.A., Alterman, M.A., Galeva, N., Larive, C.K., et al., 2004. Methanobactin, a copper-acquisition compound from methane-oxidizing bacteria. Science 305, 1612–1615.

Kirschke, S., Bousquet, P., Ciais, P., Saunois, M., Canadell, J.G., Dlugokencky, E.J., et al., 2013. Three decades of global methane sources and sinks. Nat. Geosci. 6, 813–823.

Klar, J.K., Homoky, W.B., Statham, P.J., Birchill, A.J., Harris, E.L., Woodward, E.M.S., et al., 2017. Stability of dissolved and soluble Fe(II) in shelf sediment pore waters and release to an oxic water column. Biogeochemistry 135, 49–67.

Knittel, K., Boetius, A., 2009. Anaerobic oxidation of methane: progress with an unknown process. Ann. Rev. Microbiol. 63, 311–334 (Annual Reviews, Palo Alto).

Kraal, P., Dijkstra, N., Behrends, T., Slomp, C.P., 2017. Phosphorus burial in sediments of the sulfidic deep Black Sea: key roles for adsorption by calcium carbonate and apatite authigenesis. Geochim. Cosmochim. Acta 204, 140–158.
Kraemer, S.M., Duckworth, O.W., Harrington, J.M., Schenkeveld, W.D.C., 2015. Metallophores and trace metal biogeochemistry. Aquat. Geochem. 21, 159–195.
Kulczycki, E., Fowle, D.A., Knapp, C., Graham, D.W., Roberts, J.A., 2007. Methanobactin-promoted dissolution of Cu-substituted borosilicate glass. Geobiology 5, 251–263.
Kumar, P., Nagarajan, R., Sarangi, R., 2013. Quantitative X-ray absorption and emission spectroscopies: electronic structure elucidation of Cu2S and CuS. J. Mater. Chem. C 1, 2448–2454.
Leak, D.J., Dalton, H., 1986. Growth yields of methanotrophs. Appl. Microbiol. Biotechnol. 23, 470–476.
Leal, M.F.C., Van Den Berg, C.M.G., 1998. Evidence for strong copper(I) complexation by organic ligands in seawater. Aquat. Geochem. 4, 49–75.
Luther, G.W., Tsamakis, E., 1989. Concentration and form of dissolved sulfide in the oxic water column of the ocean. Mar. Chem. 27, 165–177.
Luther, G.W., Theberge, S.M., Rozan, T.F., Rickard, D., Rowlands, C.C., Oldroyd, A., 2002. Aqueous copper sulfide clusters as intermediates during copper sulfide formation. Environ. Sci. Technol. 36, 394–402.
Mathur, R., Falck, H., Belogub, E., Milton, J., Wilson, M., Rose, A., et al., 2018. Origins of chalcocite defined by copper isotope values. Geofluids 2018, 5854829.
McCabe, J.W., Vangala, R., Angel, L.A., 2017. Binding selectivity of methanobactin from Methylosinus trichosporium OB3b for copper(I), silver(I), zinc(II), nickel(II), cobalt (II), manganese(II), lead(II), and iron(II). J. Am. Soc. Mass Spectrom. 28, 2588–2601.
Milkov, A.V., 2004. Global estimates of hydrate-bound gas in marine sediments: how much is really out there? Earth Sci. Rev. 66, 183–197.
Moffett, J.W., Dupont, C., 2007. Cu complexation by organic ligands in the sub-arctic NW Pacific and Bering Sea. Deep-Sea Res. I Oceanogr. Res. Pap. 54, 586–595.
Morse, J.W., 1994. Interactions of trace metals with authigenic sulfide minerals: implications for their bioavailability. Mar. Chem. 46, 1–6.
Murrell, J.C., 2010. The aerobic methane oxidizing bacteria (methanotrophs). In: Timmis, K.N. (Ed.), Handbook of Hydrocarbon and Lipid Microbiology. Springer Berlin Heidelberg, Berlin, Heidelberg, pp. 1953–1966.
Murrell, J.C., McDonald, I.R., Gilbert, B., 2000. Regulation of expression of methane monooxygenases by copper ions. Trends Microbiol. 8, 221–225.
Niemann, H., Losekann, T., de Beer, D., Elvert, M., Nadalig, T., Knittel, K., et al., 2006. Novel microbial communities of the Haakon Mosby mud volcano and their role as a methane sink. Nature 443, 854–858.
Ostergren, J.D., Brown, G.E., Parks, G.A., Tingle, T.N., 1999. Quantitative speciation of lead in selected mine tailings from Leadville, CO. Environ. Sci. Technol. 33, 1627–1636.
Parkman, R.H., Charnock, J.M., Bryan, N.D., Livens, F.R., Vaughan, D.J., 1999. Reactions of copper and cadmium ions in aqueous solution with goethite, lepidocrocite, mackinawite, and pyrite. Am. Mineral. 84, 407–419.
Pesch, M.L., Christl, I., Barmettler, K., Kraemer, S.M., Kretzschmar, R., 2011. Isolation and purification of Cu-free methanobactin from Methylosinus trichosporium OB3b. Geochem. Trans. 12, 9.
Pesch, M.L., Christl, I., Hoffmann, M., Kraemer, S.M., Kretzschmar, R., 2012. Copper complexation of methanobactin isolated from Methylosinus trichosporium OB3b: pH-dependent speciation and modeling. J. Inorg. Biochem. 116, 55–62.
Pesch, M.L., Hoffmann, M., Christl, I., Kraemer, S.M., Kretzschmar, R., 2013. Competitive ligand exchange between Cu-humic acid complexes and methanobactin. Geobiology 11, 44–54.
Poulton, S.W., Canfield, D.E., 2005. Development of a sequential extraction procedure for iron: implications for iron partitioning in continentally derived particulates. Chem. Geol. 214, 209–221.
Ravel, B., Newville, M., 2005. ATHENA, ARTEMIS, HEPHAESTUS: data analysis for X-ray absorption spectroscopy using IFEFFIT. J. Synchrotron Radiat. 12, 537–541.
Raven, M.R., Fike, D.A., Gomes, M.L., Webb, S.M., 2019. Chemical and isotopic evidence for organic matter sulfurization in redox gradients around mangrove roots. Front. Earth Sci. 7.
Reeburgh, W.S., 2007. Oceanic methane biogeochemistry. Chem. Rev. 107, 486–513.
Rendell, P.S., Batley, G.E., Cameron, A.J., 1980. Adsorption as a control of metal concentrations in sediment extracts. Environ. Sci. Technol. 14, 314–318.
Ruacho, A., Richon, C., Whitby, H., Bundy, R.M., 2022. Sources, sinks, and cycling of dissolved organic copper binding ligands in the ocean. Commun. Earth Environ. 3, 263.
Rudnick, R., Gao, S., 2014. Composition of the continental crust. In: Treatise on Geochemistry, vol. 4, pp. 1–51.
Rushworth, D.D., Christl, I., Kumar, N., Hoffmann, K., Kretzschmar, R., Lehmann, M.F., et al., 2022. Copper mobilisation from Cu sulphide minerals by methanobactin: effect of pH, oxygen and natural organic matter. Geobiology 20, 690–706.
Schenkeveld, W.D.C., Oburger, E., Gruber, B., Schindlegger, Y., Hann, S., Puschenreiter, M., et al., 2014a. Metal mobilization from soils by phytosiderophores – experiment and equilibrium modeling. Plant Soil 383, 59–71.
Schenkeveld, W.D.C., Schindlegger, Y., Oburger, E., Puschenreiter, M., Hann, S., Kraemer, S.M., 2014b. Geochemical processes constraining iron uptake in strategy II Fe acquisition. Environ. Sci. Technol. 48, 12662–12670.
Schenkeveld, W.D.C., Kimber, R.L., Walter, M., Oburger, E., Puschenreiter, M., Kraemer, S.M., 2017. Experimental considerations in metal mobilization from soil by chelating ligands: the influence of soil-solution ratio and pre-equilibration – a case study on Fe acquisition by phytosiderophores. Sci. Total Environ. 579, 1831–1842.
Schouten, S., van Driel, G.B., Sinninghe Damsté, J.S., de Leeuw, J.W., 1993. Natural sulphurization of ketones and aldehydes: a key reaction in the formation of organic sulphur compounds. Geochim. Cosmochim. Acta 57, 5111–5116.
Schouten, S., Wakeham, S.G., Damsté, J.S.S., 2001. Evidence for anaerobic methane oxidation by archaea in euxinic waters of the Black Sea. Org. Geochem. 32, 1277–1281.
Schubert, C.J., Coolen, M.J., Neretin, L.N., Schippers, A., Abbas, B., Durisch-Kaiser, E., et al., 2006. Aerobic and anaerobic methanotrophs in the Black Sea water column. Environ. Microbiol. 8, 1844–1856.
Seidel, H., Ehrhardt, H., Viswanathan, K., Johannes, W., 1974. Darstellung, Struktur und Eigenschaften von Kupfer(II)-Carbonat. Z. Anorg. Allg. Chem. 410, 138–148.
Shea, D., Helz, G.R., 1989. Solubility product constants of covellite and a poorly crystalline copper sulfide precipitate at 298 K. Geochim. Cosmochim. Acta 53, 229–236.
Silburn, B., Kröger, S., Parker, E.R., Sivyer, D.B., Hicks, N., Powell, C.F., et al., 2017. Benthic pH gradients across a range of shelf sea sediment types linked to sediment characteristics and seasonal variability. Biogeochemistry 135, 69–88.
Sonoda, K., Hashimoto, Y., Wang, S.-L., Ban, T., 2019. Copper and zinc in vineyard and orchard soils at millimeter vertical resolution. Sci. Total Environ. 689, 958–962.
Steeb, P., Linke, P., Treude, T., 2014. A sediment flow-through system to study the impact of shifting fluid and methane flow regimes on the efficiency of the benthic methane filter. Limnol. Oceanogr. Methods 12, 25–45.
Sunda, W.G., Price, N.M., Morel, F.M., 2005. Trace metal ion buffers and their use in culture studies. In: Algal Culturing Techniques, pp. 35–63.
Takéuchi, Y., Kudoh, Y., Sato, G., 1985. The Crystal Structure of Covellite CuS Under High Pressure Up to 33 kbar, vol. 173, pp. 119–128.
Tella, M., Bravin, M.N., Thuriès, L., Cazevieille, P., Chevassus-Rosset, C., Collin, B., et al., 2016. Increased zinc and copper availability in organic waste amended soil potentially involving distinct release mechanisms. Environ. Pollut. 212, 299–306.
Tikhonova, E.N., Tarnovetskii, I.Y., Malakhova, T.V., Gulin, M.B., Merkel, A.Y., Pimenov, N.V., 2020. Identification of aerobic methane-oxidizing bacteria in coastal sediments of the Crimean Peninsula. Microbiology 89, 740–749.
Todd, E.C., Sherman, D.M., Purton, J.A., 2003. Surface oxidation of chalcopyrite (CuFeS2) under ambient atmospheric and aqueous (pH 2-10) conditions: Cu, Fe L- and O K-edge X-ray spectroscopy. Geochim. Cosmochim. Acta 67, 2137–2146.
van Helmond, N.A.G.M., Jilbert, T., Slomp, C.P., 2018. Hypoxia in the Holocene Baltic Sea: comparing modern versus past intervals using sedimentary trace metals. Chem. Geol. 493, 478–490.
van Helmond, N.A.G.M., Robertson, E.K., Conley, D.J., Hermans, M., Humborg, C., Kubeneck, L.J., et al., 2020. Removal of phosphorus and nitrogen in sediments of the eutrophic Stockholm archipelago, Baltic Sea. Biogeosciences 17, 2745–2766.
Viollier, E., Inglett, P.W., Hunter, K., Roychoudhury, A.N., Van Cappellen, P., 2000. The ferrozine method revisited: Fe(II)/Fe(III) determination in natural waters. Appl. Geochem. 15, 785–790.
Wallenius, A.J., Dalcin Martins, P., Slomp, C.P., Jetten, M.S.M., 2021. Anthropogenic and environmental constraints on the microbial methane cycle in coastal sediments. Front. Microbiol. 12.
Walter, M., Oburger, E., Schindlegger, Y., Hann, S., Puschenreiter, M., Kraemer, S.M., et al., 2016. Retention of phytosiderophores by the soil solid phase - adsorption and desorption. Plant Soil 404, 85–97.
Whitby, H., van den Berg, C.M.G., 2015. Evidence for copper-binding humic substances in seawater. Mar. Chem. 173, 282–290.
Whitby, H., Posacka, A.M., Maldonado, M.T., van den Berg, C.M.G., 2018. Copper-binding ligands in the NE Pacific. Mar. Chem. 204, 36–48.
Whittenbury, R., Phillips, K.C., Wilkinson, J.F., 1970. Enrichment, isolation and some properties of methane-utilizing bacteria. J. Gen. Microbiol. 61, 205–218.
Zagorac, D., Muller, H., Ruehl, S., Zagorac, J., Rehme, S., 2019. Recent developments in the Inorganic Crystal Structure Database: theoretical crystal structure data and related features. J. Appl. Crystallogr. 52, 918–925.